Materials Letters 272 (2020) 127832

Contents lists available at ScienceDirect

Materials Letters

journal homepage: www.elsevier.com/locate/mlblue

Irradiation-induced swelling and hardening in HfNbTaTiZr refractory high-entropy alloy

Stanley Chang [a], Ko-Kai Tseng [b], Tzu-Yi Yang [b], Der-Sheng Chao [c], Jien-Wei Yeh [b,d], Jenq-Horng Liang [a,*]

[a] Department of Engineering and System Science, National Tsing Hua University, Hsinchu 30013, Taiwan
[b] Department of Materials Science and Engineering, National Tsing Hua University, Hsinchu 30013, Taiwan
[c] Nuclear Science and Technology Development Center, National Tsing Hua University, Hsinchu 30013, Taiwan
[d] High Entropy Materials Center, National Tsing Hua University, Hsinchu 30013, Taiwan

ARTICLE INFO

Article history:
Received 18 November 2019
Received in revised form 28 February 2020
Accepted 15 April 2020
Available online 16 April 2020

Keywords:
Refractory high-entropy alloys
Radiation damage
Nuclear materials

ABSTRACT

The lattice distortion and diffusion kinetics of refractory high-entropy alloys (RHEAs), which may be endowed with superior radiation tolerance, render RHEAs candidate materials for nuclear and aerospace systems. To investigate the irradiation behavior of body-centered cubic (BCC) RHEAs, the specimens were irradiated by 300 keV Ni^+ to a fluence of 1.5×10^{16} cm^{-2} at 100 °C, reaching a high damage level to over 30 displacements per atom (dpa). The results revealed that the swelling and hardening effects were significantly suppressed compared to those of conventional nuclear materials. Further microstructural characterization showed that the damage range far exceeded the simulated results and the range of implanted species.

1. Introduction

Clean, safe, and economical nuclear energy can help combat climate disruption opportunely. The core components operating at high temperatures in fusion and Gen IV fission reactors would be bombarded by a deluge of high-energy particles, causing severe radiation damage [1]. Refractory high-entropy alloys (RHEAs) are regarded as promising materials due to their exceptional mechanical properties under thermally-harsh environments [2]. Experimental studies using ion irradiation suggested that HEAs possess greater radiation tolerance than conventional alloys due in part to HEAs' core effects, i.e., severe lattice distortion and sluggish diffusion [3]. Furthermore, recent works attributed to HEAs' shorter phonon mean free path [4] and the broadening distribution of the vacancy and interstitial migration energy [5]. Although the irradiation behavior of face-centered cubic (FCC) structured HEAs has been examined preliminarily, only a dearth of studies has focused on that of BCC structured RHEAs with superior high-temperature mechanical properties. This study aimed to investigate the radiation-induced hardening and swelling effects in BCC HfNbTaTiZr RHEA via ion-irradiation method, which is widely adopted to efficiently examine materials' irradiation behavior [6].

2. Experimental procedures

The HfNbTaTiZr RHEA was prepared by vacuum-arc-melting of high-purity elements (99.9 wt%). Melting was repeated five times to enhance the chemical homogeneity. The ingots were cold-rolled by 70%, then homogenized in a vacuum quartz tube at 1200 °C for 15 min, followed by water quench [7]. Samples were cut into a size of 1 × 1 × 0.3 cm and then mechanically polished to achieve roughness below 2 nm. The nearly equiatomic composition before and after the irradiation (Hf: 19.7 ± 0.7%; Nb: 21.0 ± 0.8%; Ta: 20.4 ± 0.9%; Ti: 19.2 ± 0.8%; Zr: 19.7 ± 0.7%) was confirmed by energy-dispersive X-ray spectroscopy (EDS) via a JEOL-IT100.

The samples were irradiated with 300 keV Ni^+ to a fluence of 1.5×10^{16} cm^{-2} at 100 °C using an LC-4 ion-implanter. The reason for using face-centered cubic (FCC) Nickel ions irradiation, rather than choosing one of the elements in BCC HfNbTaTiZr alloy, is to facilitate implantation profile analysis and to observe whether special damages would occur to the BCC RHEA. Cu foil was used to partially masked the surface of the samples during the ion irradiation, leaving pristine regions for convenient comparison with irradiated counterparts. The damage and implantation profile was simulated by the Stopping and Range of Ions in Matter-2013 (SRIM) software in "Quick" Kinchin–Pease mode with a displacement threshold energy of 90, 60, 90, 30, and 40 eV respectively for Hf, Nb, Ta, Ti, and Zr. [8]. Note that the actual density of HfNbTaTiZr was reported to be 9.94 g/cm^3 [9] and the lattice binding energy levels

* Corresponding author.
E-mail address: jhliang@ess.nthu.edu.tw (J.-H. Liang).

https://doi.org/10.1016/j.matlet.2020.127832
0167-577X/

of the five elements were set to be zero. The dpa levels were computed by SRIM according to the method published in reference [10]. The depth profile of the implanted Ni^+, as well as the five elements in HfNbTaTiZr RHEA, was measured using secondary ion mass spectrometry (SIMS) via a TOF-SIMS V to compare with the SRIM-simulated results.

The nanoindentation was carried out on a Hysitron TI 980 Triboindenter with a Berkovich tip under quasi-static mode to measure the hardness of the samples before and after the irradiation. The nominal maximum indentation depth was controlled at 100 nm to avoid the substrate effect and to ensure that the plastically deformed zone could cover the irradiated layer. The step height between the elevated irradiated region and the adjacent Cu-foil-masked surface was measured by a Bruker Dimension ICON scanning probe microscope (SPM). The volume swelling was then calculated to be the height difference divided by the depth of damaged region, based on the ASTM standard E521-16 [11]. The microstructure of HfNbTaTiZr alloy was examined by a JEOL JEM-F200 transmission electron microscope (TEM) operated at 200 keV. In-situ focused ion beam (FIB) lift-out techniques were used for the preparation of TEM samples via a TESCAN GAIA3.

3. Results and discussion

3.1. SRIM & SIMS analysis

Fig. 1(a) shows the SRIM-predicted results under a Ni^+ fluence of 1.5×10^{16} cm^{-2}. The damage range is roughly 300 nm and the peak damage level is over 30 dpa. Fig. 1(b) presents the SIMS-measured depth profiles of Ni and the five elements of HfNbTaTiZr RHEA in the as-irradiated sample. The range of implanted Ni^+ agrees with the SRIM simulation. The actual Ni distribution is flatter because SRIM does not take account of the temperature effect, whereas the implantation stage was held at 100 °C. The samples' temperature might also rise as the Ni^+ heavily bombarded the target atoms. The implanted Ni would then diffuse and distribute broader, similar to the effect of annealing. The five elements in the HfNbTaTiZr RHEA distribute evenly with depth, indicating that the irradiation did not induce phase transformation, which was further corroborated by TEM analysis shown later. Note that the peaks near the surface may result from the shallow oxidized layer as O_2^+ was used for the SIMS sputtering. The interference of high-concentration Ni approximately before 150 nm may lead to the slightly lower outlines of the other five elements.

3.2. Irradiation swelling and hardening

Fig. 2 shows the average step height of 3.7 ± 0.1 nm across the irradiated and pristine areas by the 32-line scans of SPM. According to the SRIM-simulated results, the damage depth was chosen to be 300 nm. The swelling ratio can be estimated to be 1.23 ± 0.03%. Compared to conventional nuclear materials, HfNbTaTiZr RHEA exhibits similar excellent swelling resistance to the FCC $Al_{0.1}$-CoCrFeNi HEA [12]. Note that the peak at the boundary of the irradiated and pristine surface may result from the accumulation of target atoms alongside the Cu foil when the sample swelled during the irradiation. The nanoindentation tests showed the overlapped hardness values of 3.6 ± 0.3 and 3.5 ± 0.4 GPa at the irradiated and pristine areas respectively, indicating that the hardening effect is almost indistinguishable yet with high-dpa damage extent.

3.3. TEM characterization

Fig. 3(a) presents the low-magnification TEM image of the irradiated HfNbTaTiZr RHEA. Defect clusters indicated by the black spots stretched to over 500 nm from the surface, far exceeding the SRIM predicted depth even though the implanted Ni^+ stopped at roughly 300-nm as confirmed by SIMS. Fig. 3(b)–(d) present

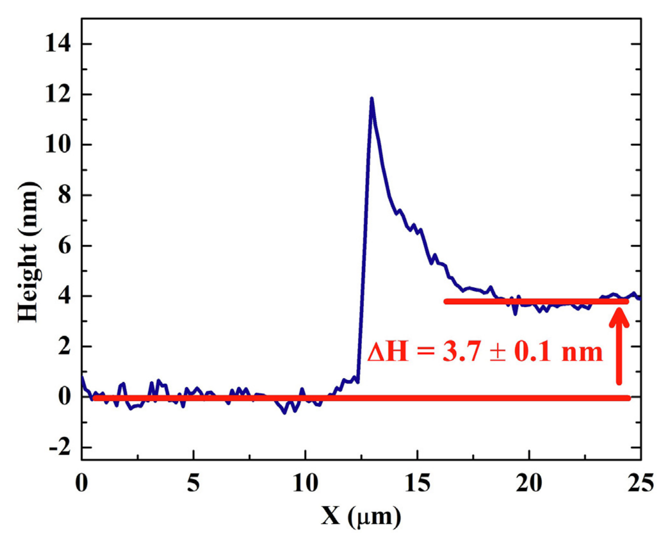

Fig. 2. The average step height profile across the boundary of the irradiated and pristine surface measured by SPM.

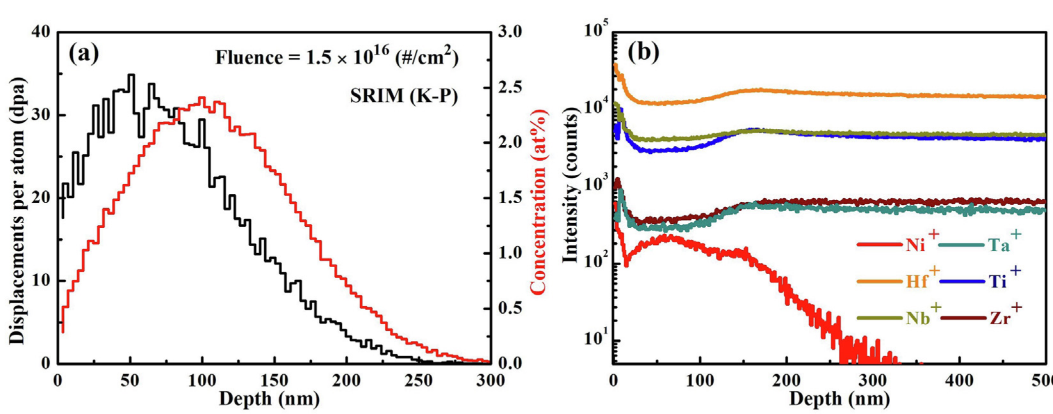

Fig 1. (a) SRIM-simulated damage profile and ion distribution of 300 keV Ni^+ implanted into HfNbTaTiZr with a fluence of 1.5×10^{16} cm^{-2}; (b) SIMS-measured depth profiles of Ni^+, Hf^+, Nb^+, Ta^+, Ti^+, and Zr^+ in the as-irradiated HfNbTaTiZr RHEA.

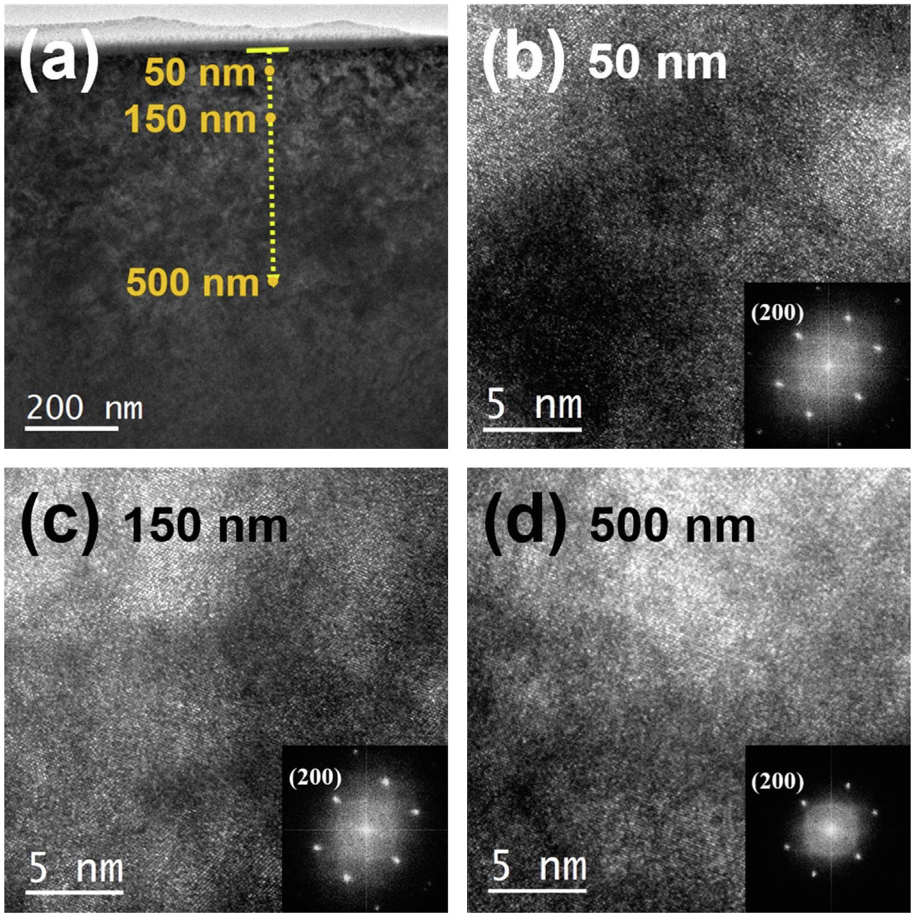

Fig. 3. (a) Low-magnification TEM image of the irradiated HfNbTaTiZr RHEA; high-resolution TEM images with FTT diffraction pattern taken at a depth of (b) 50 nm, (c) 150 nm, and (d) 500 nm.

respectively the high-resolution TEM images with fast Fourier transform (FFT) diffraction pattern taken at a depth of 50, 150, and 500 nm. Fewer defects were observed at a deeper depth as shown in Fig. 3(a) and Fig. 3(d) with clearer diffraction pattern. These defect clusters may lead to the modest swelling evidenced by SPM. Note that damage range significantly depends on ion fluence, and SRIM simulations may fail to predict the real damage range, especially for high-fluence ion-irradiation [13]. The depth for calculating the swelling ratio was the simulated damage range as adopted by some other similar studies, rather than the actual depth of irradiation-induced defects observed from TEM. Therefore, the swelling ratio was overestimated in this study and could be the same case for some literature. Furthermore, chemical complexity can impact defect evolution [13]. Future work should examine and compare the damage evolution with different ion-irradiation fluences and the number of constituent elements in equiatomic alloys.

4. Conclusions

The HfNbTaTiZr RHEA was irradiated at 100 °C with 300 keV Ni^+ to over 30 dpa. Modest irradiation-induced swelling was observed. The nanoindentation hardness after the irradiation was almost unchanged. The damage range extended much deeper than the SRIM-simulated depth and the Ni^+ implanted range. No phase transformation can be found in the BCC HfNbTaTiZr RHEA bombarded by a significant amount of FCC Ni^+. HfNbTaTiZr RHEA exhibits excellent overall radiation tolerance against high-dosage damage in this study. Future work should study the damage evolution of equiatomic alloys with different irradiation fluences and chemical complexity.

CRediT authorship contribution statement

Stanley Chang: Conceptualization, Methodology, Investigation, Software, Visualization, Formal analysis, Writing - original draft, Writing - review & editing, Data curation. **Ko-Kai Tseng:** Methodology, Investigation, Formal analysis, Writing - review & editing, Resources. **Tzu-Yi Yang:** Investigation, Formal analysis. **Der-Sheng Chao:** Writing - review & editing. **Jien-Wei Yeh:** Resources, Funding acquisition. **Jenq-Horng Liang:** Supervision, Funding acquisition.

Declaration of Competing Interest

The authors declare that they have no known competing financial interests or personal relationships that could have appeared to influence the work reported in this paper.

Acknowledgments

The authors appreciate the financial support by the "High Entropy Materials Center" from The Featured Areas Research Center Program within the framework of the Higher Education Sprout Project by the Ministry of Education (MOE) and the Project MOST

109-2634-F-007-024- by Ministry of Science and Technology (MOST) in Taiwan.

References

[1] S.J. Zinkle, G.S. Was, Materials challenges in nuclear energy, Acta Mater. 61 (3) (2013) 735–758, https://doi.org/10.1016/j.actamat.2012.11.004.
[2] Senkov, D.B. Miracle, K.J. Chaput, J.-P. Couzinie, Development and exploration of refractory high entropy alloys—A review, J. Mater. Res. 33 (19) (2018) 3092–3128, https://doi.org/10.1557/jmr.2018.153.
[3] Y. Zhang, S. Zhao, W.J. Weber, K. Nordlund, F. Granberg, F. Djurabekova, Atomic-level heterogeneity and defect dynamics in concentrated solid-solution alloys, Curr. Opin. Solid State Mater. Sci. 21 (5) (2017) 221–237, https://doi.org/10.1016/j.cossms.2017.02.002.
[4] F. Granberg, K. Nordlund, M.W. Ullah, K. Jin, C. Lu, H. Bei, L.M. Wang, F. Djurabekova, W.J. Weber, Y. Zhang, Mechanism of radiation damage reduction in equiatomic multicomponent single phase alloys, Phys. Rev. Lett. 116 (13) (2016), https://doi.org/10.1103/PhysRevLett.116.135504 135504.
[5] C. Lu et al., Enhancing radiation tolerance by controlling defect mobility and migration pathways in multicomponent single-phase alloys, Nat. Commun. 7 (2016) 13564, https://doi.org/10.1038/ncomms13564.
[6] G.S. Was, Emulating neutron irradiation effects with ions, in: G.S. Was (Ed.), Fundamentals of Radiation Materials Science, Springer, New York, NY, 2017, pp. 631-665.
[7] C.C. Juan, M.H. Tsai, C.W. Tsai, W.L. Hsu, C.M. Lin, S.K. Chen, S.J. Lin, J.W. Yeh, Simultaneously increasing the strength and ductility of a refractory high-entropy alloy via grain refining, Mater. Lett. 184 (2016) 200–203, https://doi.org/10.1016/j.matlet.2016.08.060.
[8] G.S. Was, The displacement of atoms, in: G.S. Was (Ed.), Fundamentals of Radiation Materials Science, Springer, New York, NY, 2017, pp. 77-130.
[9] J.M. Senkov, S.V. Scott, D.B. Senkova, C.F. Miracle, Woodward, Microstructure and room temperature properties of a high-entropy TaNbHfZrTi alloy, J. Alloys Compd. 509 (2011) 6043–6048, https://doi.org/10.1016/j.jallcom.2011.02.171.
[10] R.E. Stoller, M.B. Toloczko, G.S. Was, A.G. Certain, S. Dwaraknath, F.A. Garner, On the use of SRIM for computing radiation damage exposure, Nucl. Instrum. Methods Phys. Res. 310 (2013) 75–80, https://doi.org/10.1016/j.nimb.2013.05.008.
[11] E521-16 Standard Practice for Investigating the Effects of Neutron Radiation Damage Using Charged-Particle Irradiation, ASTM International, West Conshohocken, PA, 2016.
[12] S.Q. Xia, X. Yang, T.F. Yang, S. Liu, Y. Zhang, Irradiation resistance in $Al_xCoCrFeNi$ high entropy alloys, JOM 67 (10) (2015) 2340–2344, https://doi.org/10.1007/s11837-015-1568-4.
[13] C. Lu et al., Direct observation of defect range and evolution in ion-irradiated single crystalline Ni and Ni binary alloys, Sci. Rep. 6 (2016) 19994, https://doi.org/10.1038/srep19994.